

THE HADRONIC PICTURE OF THE PHOTON

THORSTEN WENGLER

CERN, EP division, CH-1211 Geneve 23, Switzerland

email: Thorsten.Wengler@cern.ch

The hadronic interactions of the photon are studied in terms of new measurements of the total hadronic cross section and di-jet production in photon-photon collisions at LEP2.

1 Total hadronic $\gamma\gamma$ cross section

The reaction of $e^+e^- \rightarrow e^+e^- \gamma^*\gamma^* \rightarrow e^+e^- + \text{hadrons}$ is analysed for quasi-real photons using data collected by L3 and OPAL at LEP2. From this measurement the total hadronic cross section $\sigma_{\gamma\gamma}(W)$ is extracted using a luminosity function for the photon flux and extrapolating to $Q^2=0$ GeV². The L3 data ¹ are shown in Figure 1, representing an integrated luminosity of 392.6 pb⁻¹ taken at \sqrt{s} from 189 to 202 GeV. The total hadronic cross section, $\sigma_{\gamma\gamma}$, is shown as a function of the invariant mass W of the photon-photon system. Also shown as the solid line is the result of a fit using the parameterisation proposed by Donnachie and Landshoff ²: $\sigma_{\text{tot}} = As^\epsilon + Bs^{-\eta}$. The second term represents the Reggeon exchange dominant at low W , while at high W the Pomeron exchange driven by the exponent ϵ prevails. If photons behave predominantly like hadrons the values of $\epsilon = 0.095 \pm 0.002$ and $\eta = 0.34 \pm 0.02$ obtained from a universal fit to hadron-hadron cross sections ³ should be valid for $\sigma_{\gamma\gamma}(W)$ as well. Indeed this is not the case for the L3 data, as demonstrated by the dashed line in Figure 1. Instead a fit with A, B, and ϵ as free parameters yields $\epsilon = 0.250 \pm 0.016$, which is more than a factor of two higher than the universal value, a rise significantly steeper than expected from the universal fit of hadron-hadron cross sections. The L3 data is compared to an OPAL measurement ⁴ using an integrated luminosity of 74.3 pb⁻¹ taken at \sqrt{s} from 161 to 183 GeV. Both measurements are consistent

inside their respective uncertainties. A similar fit as described above to the OPAL data however yields $\epsilon = 0.101 \pm 0.025$, in agreement with the universal fit. The steeper rise observed by L3 is mainly determined by their data points at highest and lowest W .

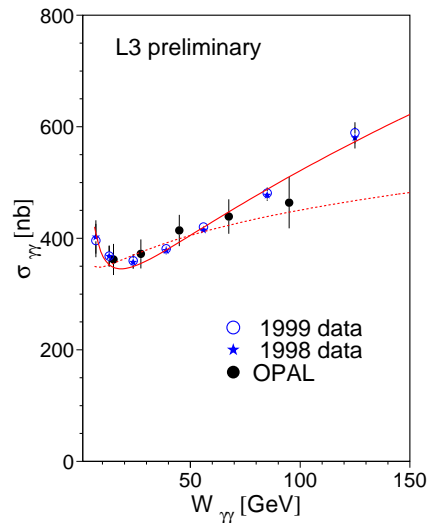


Figure 1. The photon-photon total hadronic cross section, $\sigma_{\gamma\gamma}(W)$. The solid line is a fit to the L3 data, the dashed line uses the parameters from a universal fit to hadron-hadron cross sections (see text). Here the L3 points do not include the dominant systematic error due to MC model dependencies. With this error included the total uncertainties on the OPAL and L3 measurements are of comparable size.

2 Di-jet Production

The production of di-jets in the collisions of two quasi-real photons has been measured by ALEPH and OPAL. Jet production is calculable in perturbative QCD. The measurements can therefore be used to study the per-

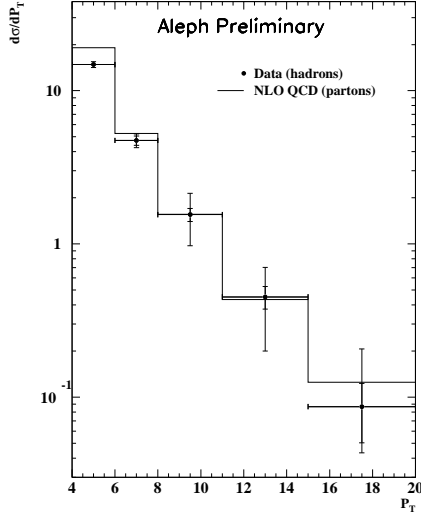


Figure 2. Differential di-jet cross section as measured by ALEPH using 59.2 pb^{-1} taken at $\sqrt{s} = 183 \text{ GeV}$.

formance of NLO predictions for these processes. ALEPH ⁵ has analysed 59.2 pb^{-1} taken at $\sqrt{s} = 183 \text{ GeV}$ using the Durham k_{\perp} clustering algorithm ⁶ with $Y_{\text{cut}} = 0.018$, chosen to maximise the rate of di-jet events. Di-jet events are required to have at least two jets with $|\eta_{\text{jet}}| < 1.4$, and a minimum jet transverse momentum of 4 (3) GeV for the first (second) jet. The differential di-jet cross section as a function of the highest p_T jet in the event is shown in Figure 2. The data is compared to an NLO calculation of Klasen et al.⁷, performed at the level of QCD partons. The agreement of the calculation with the data is good, except at the lowest p_T^{jet} .

OPAL ⁸ has analysed 384 pb^{-1} taken at \sqrt{s} from 189 GeV to 202 GeV. Jets are found using the inclusive k_{\perp} ⁶ clustering algorithm. Jets entering the analysis have a pseudorapidity $|\eta_{\text{jet}}| < 2.0$. The two jets with the highest E_T^{jet} in each event are taken. An average transverse energy of the two leading jets in the event of $\bar{E}_T^{\text{jet}} > 5 \text{ GeV}$ is required. The additional condition $|E_{T,1}^{\text{jet}} - E_{T,2}^{\text{jet}}| / (E_{T,1}^{\text{jet}} + E_{T,2}^{\text{jet}}) < 1/4$ keeps low E_T^{jet} jets from entering the distributions and ensures asymmetric E_T^{jet} thresholds for the two jets. The differ-

ential cross section as a function of \bar{E}_T^{jet} (not shown) is reasonably well described by both the LO MC models PHOJET and PYTHIA and the NLO calculation ⁷. Di-jet events have the particular advantage that the fraction of the photon momentum, x_{γ} , entering the hard scattering can be estimated from the di-jet system. The observable quantity $x_{\gamma}^{\pm} \equiv (\sum_{\text{jets}=1,2} (E \pm p_z)) / (\sum_{\text{hadrons}} (E \pm p_z))$ is defined for this purpose. OPAL has for the first time measured differential cross sections as a function of x_{γ} , where the data has been fully unfolded for detector effects. Here x_{γ} refers to both x_{γ}^{+} and x_{γ}^{-} entering the distribution. The region of small x_{γ} is expected to be dominated by resolved photon interactions, and is hence particularly sensitive to the gluon density in the photon. The OPAL data is shown in Figure 3 in three regions of \bar{E}_T^{jet} . The data is compared to three predictions of the PHOJET generator using the GRV LO, SaS1D, and LAC1 parton distribution functions respectively. The sensitivity of this observable to the different parton distributions is clearly visible. The already disfavoured LAC1 set is shown to demonstrate the effect of a high gluon density and clearly overshoots the data especially at low \bar{E}_T^{jet} . GRV and SaS1D on the other hand seem to underestimate the gluon density. A preliminary study of the underlying event us-

	data [pb]	NLO [pb]
$5 \text{ GeV} < \bar{E}_T^{\text{jet}} < 7 \text{ GeV}$		
$x_{\gamma} > 0.75$	111.0 ± 3.8	206.5
$x_{\gamma} < 0.75$	205.5 ± 4.8	84.4
$7 \text{ GeV} < \bar{E}_T^{\text{jet}} < 11 \text{ GeV}$		
$x_{\gamma} > 0.75$	77.4 ± 2.6	87.0
$x_{\gamma} < 0.75$	71.5 ± 2.2	32.6
$11 \text{ GeV} < \bar{E}_T^{\text{jet}} < 25 \text{ GeV}$		
$x_{\gamma} > 0.75$	32.0 ± 2.5	27.4
$x_{\gamma} < 0.75$	15.8 ± 1.7	7.5

Table 1. OPAL di-jet cross sections compared to NLO predictions in regions of x_{γ} and \bar{E}_T^{jet} .

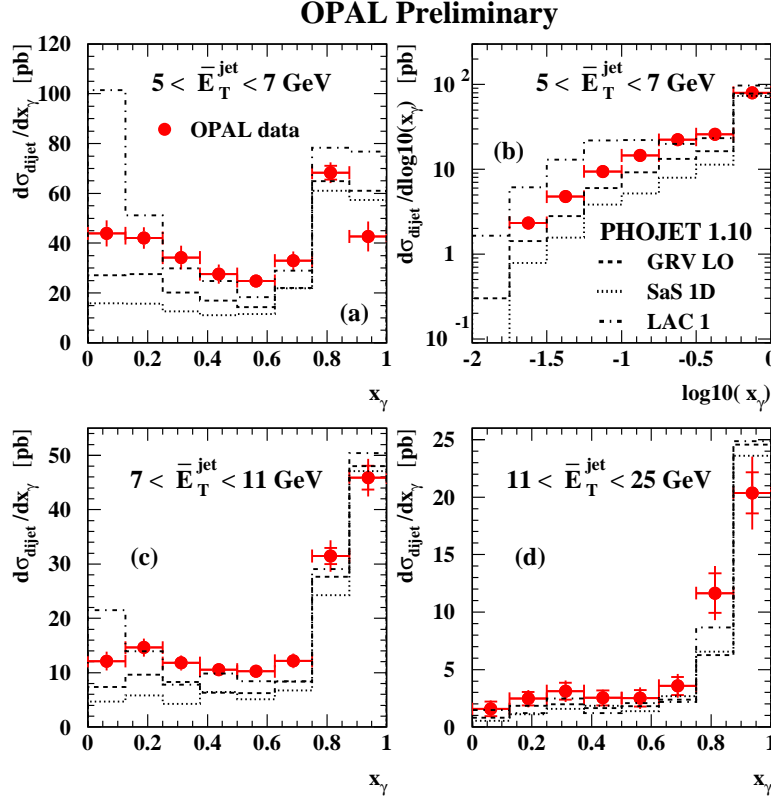


Figure 3. OPAL differential di-jet cross section as a function of x_γ in several regions of \bar{E}_T^{jet} .

ing PYTHIA with and without multiple interactions show a visible effect only at the lowest values of \bar{E}_T^{jet} and x_γ . Table 1 compares the OPAL measurement with an NLO calculation⁷ for small and large x_γ in the three regions of \bar{E}_T^{jet} . It should be stressed that hadronisation corrections are not taken into account in this calculation. The NLO calculation predicts much too large a cross section for $x_\gamma > 0.75$ and small \bar{E}_T^{jet} , while being too low by about a factor of two for $x_\gamma < 0.75$. With increasing \bar{E}_T^{jet} the discrepancy for $x_\gamma > 0.75$ largely disappears, while for $x_\gamma < 0.75$ the NLO prediction remains too low by a factor of two for the highest $x_\gamma > 0.75$ considered. This also suggests that the parton density functions used in the NLO calculation (GRV) underestimate the gluon density in the photon.

References

1. L3 Coll., L3 note 2570, Abstract 622 submitted to this conference.
2. A. Donnachie and P.V. Landshoff, Phys. Lett. B296 (1992) 227.
3. PDG, Eur. Phys. J. C3 (1998) 1.
4. Opal Coll., G. Abbiendi et al., Eur. Phys. J. C14 (2000) 199.
5. ALEPH Coll., ALEPH 2000-052, Abstract 265 submitted to this conference.
6. S. Catani, Yu.L. Dokshitzer, M.H. Seymour and B.R. Webber, Nucl. Phys. B406 (1993) 187; S.D. Ellis, D.E. Soper, Phys. Rev. D48 (1993) 3160
7. M. Klasen, T. Kleinwort and G. Kramer, Eur. Phys. J. Direct C1 (1998) 1; M. Klasen, private communication.
8. OPAL Coll., OPAL PN443, Abstract 583 submitted to this conference.